

Light Induced Further Agglomeration of Metal Particles

Yi Zhang and Claire Gu

Department of Electrical Engineering, University of California, Santa Cruz, CA 95064

Phone: (831) 459-4716

Fax: (831) 459-4829

claire@ee.ucsc.edu

Adam M. Schwartzberg, Shaowei Chen and Jin Z. Zhang

Department of Chemistry, University of California, Santa Cruz, CA 95064

ABSTRACT

The observation of an unusual light-induced agglomeration phenomenon that occurs besides the trapping of the gold nanoparticles aggregates (GNAs) has been observed. The observed agglomerate has a 60-100 μm donut-shaped metal microstructure with the rate of formation dependent on the laser power used. In this paper, the forces involved and the mechanism of this further agglomeration phenomenon are analyzed in detail. The observed trapping can partially be explained by a model including the optical radiation force and radiometric force. However, the light-induced agglomeration cannot be explained by optical trapping alone as the size of the agglomerate is much greater than the waist of the Gaussian beam used in the optical trapping. Hydrodynamic drag force induced by the laser heating is also considered to play a role. Besides these forces, the mechanism of light-induced agglomeration is attributed to ion detachment from the surface of the nanoparticles/aggregates due to light illumination or heating. This is supported by the observation of reversible conductivity changes in the nanoparticle/aggregate solution upon laser illumination or direct heating. Light-induced agglomeration can be useful in the design and fabrication of microstructures from nanomaterials for various device applications.

Keywords: Optical trapping, surface enhanced Raman scattering (SERS), nanoparticle aggregates, hydrodynamic drag forces

1. Introduction

Metal nanoparticles have attracted significant attention recently due to their unique optical,¹⁻⁴ chemical,^{5,6} and other physical properties.⁷⁻⁹ Gold and silver particles are of particular interest due to their potential applications in various areas including surface enhanced Raman scattering (SERS).¹⁰⁻¹⁵ SERS possesses the molecular specificity of Raman scattering, while magnifying the nominally weak signal by as much as ten orders of magnitude due to the greatly enhanced electromagnetic field at the surface of the nanoparticles upon resonant excitation.¹⁶⁻¹⁹ It has been found that the majority of the enhancement takes place at the junction of aggregated particles²⁰⁻²³ bringing to light the importance of interparticle interaction, in particular, under photoirradiation.

Recently, we have shown that surface chemistry is an important factor in nanoparticles aggregation that affects the physical properties of the aggregates.^{5,6} Stable nanoparticles solution require a repulsive surface capping layer of ions or molecules. If the capping layer is interrupted, nanoparticles will form aggregates. This can be induced experimentally in several ways. The most common aggregation method for SERS studies is the addition of sodium chloride or pyridine to silver or gold nanoparticles stabilized by negatively charged citrate ions. Sodium chloride induces aggregation by screening surface charges, while neutral pyridine displaces the charged citrate and decreases particle-particle repulsion. Aggregation or agglomeration is a dynamic process that depends sensitively on many factors such as light, heat, embedding environment, and, most importantly, the chemical nature of the surface capping ions or molecules. Recently, we observed that with a high power laser beam focused on a single GNA, a huge donut-shaped agglomerate was formed²⁴, which proved that the light and light induced heat could affect surface chemistry of the GNAs and contribute to the dynamic process of agglomeration. However, the interplay among these factors and their effects on the aggregation of nanoparticles need further investigation.

Optical trapping^{25, 26} is a promising technique for probing the fundamental properties of metal nanoparticles/aggregates and for enhancing SERS detection in chemical and biochemical analysis.²⁷ Optical trapping of nanometer-sized Rayleigh ($\phi \ll \lambda$, where ϕ is the size of the particle and λ is the wavelength of the trapping light) metal particles^{28, 29} has been achieved in three dimensions using TEM₀₀ beams. However, micron-sized metal Mie particles^{30, 31} ($\phi \gg \lambda$) can only be trapped in two dimensions with the light focused below the center of the particle (FIG 1) with TEM₀₀ beams. Three dimensional trapping of Mie metal particles had been achieved in a TEM₀₁-mode trapping beam or an obstructed laser beam, where the ring-shaped intensity profile increases the axial trapping efficiency.³²⁻³⁴

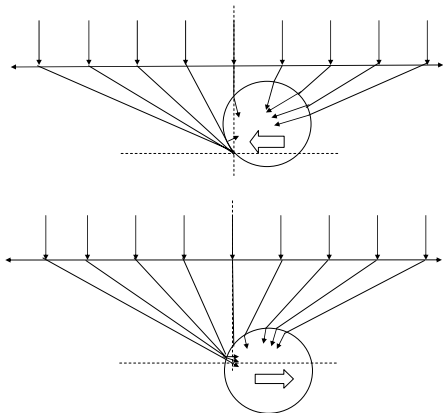


FIG 1. Two different configurations of light focused on the spherical metal particle. The optical radiation force exerted on the metal particle, indicated by the small arrows pointing to the center inside the sphere. (a) The focal plane is below the center of the metal particles and a net attractive force is generated to pull the particle to the focus. (b) The focal plane is above the center of the metal particle and a repulsive force is generated to push the particle out of the focus (adopted from Ref. 29).

operation. We attribute the additional cause for the observed agglomeration to an optical or thermal detachment of ions from the nanoparticle/aggregate surface.

When optical tweezers are used to trap particles, heat can be generated due to light absorption. As a result, the GNAs can be heated to high temperatures, especially at the laser focus and when the nanoparticles have strong absorption at the laser wavelength. This light-induced heating will result in the ion dissociation from the GNAs surface. This suggestion is supported by an independent study of reversible changes of the electrical conductivity of the nanoparticle/aggregate solution upon laser illumination or direct heating. Furthermore, with a high power laser beam focused on the GNAs, the surrounding water solution will be heated and possibly vaporized, resulting in a hydrodynamic drag force. In this paper we will include various heat-related forces in our analysis.

2. Experimental method

A. Nanoparticle Synthesis

GNAs were synthesized by the method of Schwartzberg *et al.*⁵ Briefly, 500 μl of a 0.02 M HAuCl₄ stock solution was diluted to 5×10^{-4} M with Milli-Q water in glassware cleaned in aquaregia and rinsed with Milli-Q water to avoid contamination. To this, 40 - 60 μl of a 0.1 M solution of Na₂S aged 2-3 months was added. After approximately 60-120 minutes, the color changed from a straw yellow to deep purple with the extended plasmon band (EPB) growing

Optical trapping force has been analyzed in detail in conjunction with the applications of optical tweezers. When a particle is near the focus of a Gaussian beam, it experiences a repulsive scattering force and an attractive gradient force simultaneously.²⁵ When the two forces balance each other out, the particle will be trapped. Two theoretical models have been developed to evaluate the trapping force, based on ray optics^{25, 32} and electromagnetic wave theory³⁴⁻³⁶, respectively. Both models agree with experimental measurements of dielectric Rayleigh and Mie particles. In the case of trapping micron-sized metal particles, both models could be used but ray optics is more suitable for analyzing the radiation force due to the large particle size.

An interesting phenomenon-light can induce further agglomeration of the aggregates has been observed.²⁴ During the process of forming this agglomerate, there are two processes, first, aggregates tens of micrometers away are attracted to beam, second, stable donuts shaped aggregate is formed. The mechanism of forming further aggregation has been introduced in great detail.²⁴ But the analysis of the forces are still left blank and not fully explored. Optical trapping can be partially explained by a model based on the radiation force and radiometric force, the light-induced agglomeration indicates an additional mechanism in

in between 600-1000 nm, indicating reaction completion. The aggregate formation is signified by a strong NIR absorption band at wavelengths longer than 600 nm. This synthesis yields gold aggregates capped with sulfur-oxygen species, the nature of which is not entirely known. However, it is believed that these species not only stabilize the particles, but also induce stable aggregation.

Gold nanoparticles of approximately 40 nm were synthesized by the Turkevich method,³⁸ and silver nanoparticles were synthesized by the Lee method.³⁹ These procedures involve the reduction of metal salts by sodium citrate in a boiling aqueous solution resulting in citrate capped nanoparticles

B. Optical Trapping and Light Induced Aggregation

The instruments used for optical trapping have been introduced with great detail before²⁴. Briefly, a CW Verdi laser at 532 nm with a maximum laser power of 2 W was used in the experiment as the trapping light source. The diameter of the laser beam was reduced before entering the 60× objective lens (Numerical Aperture =0.85), however, the effective Numerical Aperture (NA) was 0.64 because the objective lens was pointed into the water solution (with GNAs). The trapping and agglomeration were observed with a CCD camera mounted behind a cubic beam splitter. Another lens (f=10 cm) was placed in front of the camera in order to observe the image at the focus of the objective lens.

C. Electrical Conductivity Measurement

Same experiment setup²⁴ was used to measure the electrical conductivity of the GNAs solution. Briefly, the electrical conductivity of GNAs solution was measured under various conditions with a computer-controlled potentiostat (SI-1280B). Two gold electrodes were inserted into the GNAs solution with a spacing of 2 cm and an external 3 V potential was applied. The electrodes were about 2 cm long and the diameter was about 1 mm with a tip diameter of 50 μm. About 75% of the entire electrode was immersed into the solution. A thermometer was also inserted into the solution between the electrodes to trace the temperature change of the solution.

At first, the sample was illuminated with another CW Verdi laser with an output power 3 W at 532 nm between the electrodes with constant stirring to insure thermal consistency throughout the solution. Afterwards, the solution was cooled down back to its original temperature. Next, the solution was heated with a hot plate without laser light. The current change was recorded as a function of time in the cases of both laser illumination and direct heating.

3. Experimental results

A. UV-Visible Spectrum and TEM of Gold Nanoparticles/Aggregates

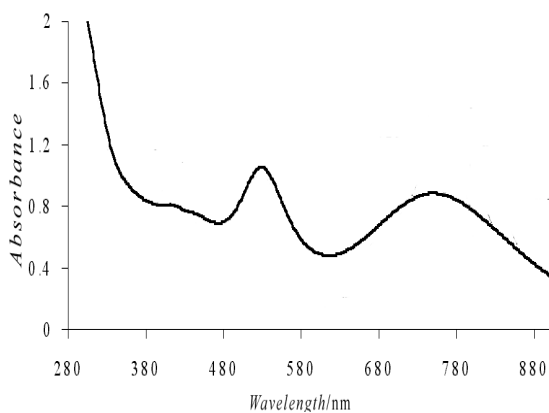


FIG 2. UV-Visible absorption spectrum of gold nanoparticle aggregate solution. Concentration is as prepared and as used in trapping experiments.

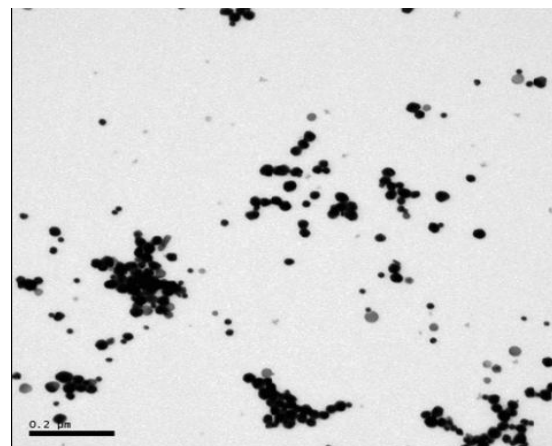


FIG 3. A representative TEM image of aggregates formed by ~10 nm gold nanoparticles, a variety of aggregate sizes and shape are shown.

The UV-Visible electronic absorption spectrum (FIG 2) of the GNA shows two bands in the visible to near IR region, one peaked at 530 nm and another near 760 nm. The 530 nm band is the transverse surface plasmon absorption, typical for gold nanoparticles, while the 760 nm band has been attributed to strong interaction between nanoparticles in the aggregates, termed extended plasmon band (EPB).³⁹ The width and location of the EPB strongly depends on the size and the shape of the aggregates.

Representative TEM images of the GNA are shown in FIG 3. Based on the TEM, the average size of the aggregates varies from 100 nm to over 2000 nm and each aggregate is composed of gold nanoparticles with an average diameter between 5-10 nm.

B. Observation of Optical Trapping of Nanoparticles/Aggregates

The observed optical trapping of a single GNA has been introduced before²⁴. Same experiment was repeated here. Briefly, a 2 μm in diameter, GNA was trapped stably in two dimensions. Larger cylindrical, elliptical, or spherical aggregates up to 3 μm were also trapped with a TEM_{00} mode laser beam (532 nm) with approximately 50 mW power and a beam waist of about 1 μm . The micron-sized metal structure could only be trapped in the periphery of the beam when focused at the bottom of the aggregate (FIG 4).

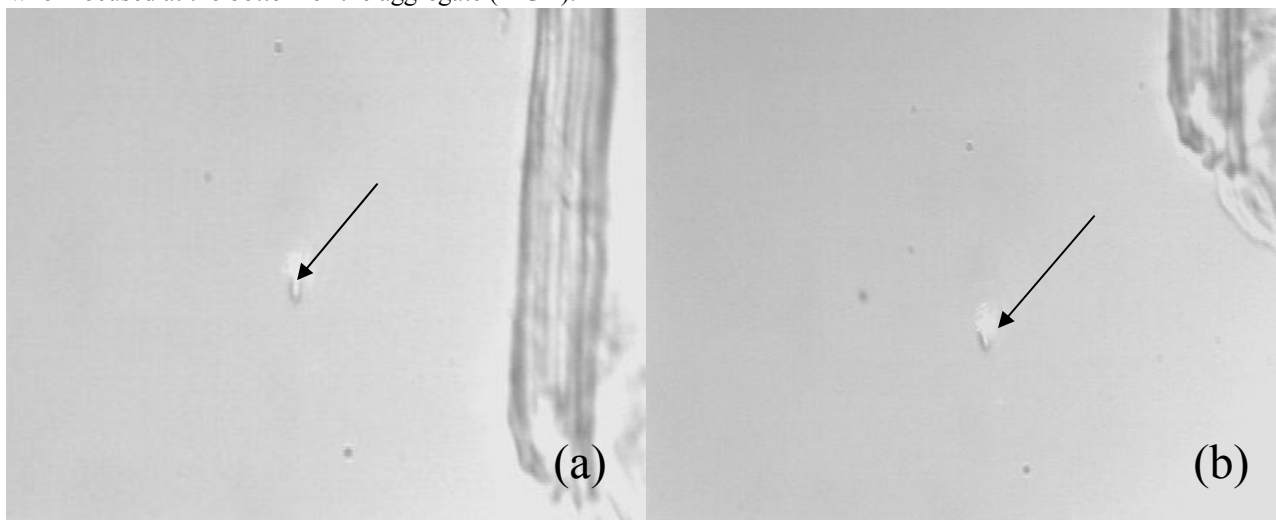


FIG 4. Microscopic images of a two-dimensionally trapped GNA (approximately 2 μm) by using a fixed Verdi laser beam of TEM_{00} mode (a) before and (b) after the movement of the glass slide. The arrow points to the darker aggregate trapped at the periphery of the beam. The bright spot is the laser focus which is not totally filtered out. The big bar-shaped object on the right is presented as the reference spot.

Although our experimental setup does not allow direct observation of trapping of individual isolated gold or silver nanoparticles with size smaller than a few hundred nm since they are much smaller than the diffraction limit of the experimental system, we did observe trapping of aggregates with regular shapes and diameters about 1-2 μm that were formed from the isolated particles. The mechanism for aggregation is believed to be largely caused by light or heat-induced ion detachment, as discussed next.

C. Observation of Light Induced Aggregation

Agglomeration of the GNAs was observed under the illumination of a strong laser beam. Previously, we reported the formation of elliptical donut-shaped agglomerate when using a cylindrical lens in our system.²⁴ Here, we study the effect of the laser beam shape by replacing the cylindrical lens by a convex lens to form a circular shaped laser spot. The light-induced agglomeration only took place at some particular locations, where the GNAs about 1-2 μm are deposited on the glass slide. The agglomeration occurred more quickly for larger sized aggregates, e.g. in the 1-2 μm range. FIG 4a shows images of the agglomeration process. Typically, some aggregates were first attracted and trapped close to the focus region of the laser beam (as what happened in FIG 4), since the metal particles could not be stably trapped in the focus and the particles would be pushed away to the peripheral region. Within 10-15 seconds, more aggregates were attracted to the laser beam and collected in the peripheral region of the laser beam (FIG 5b).

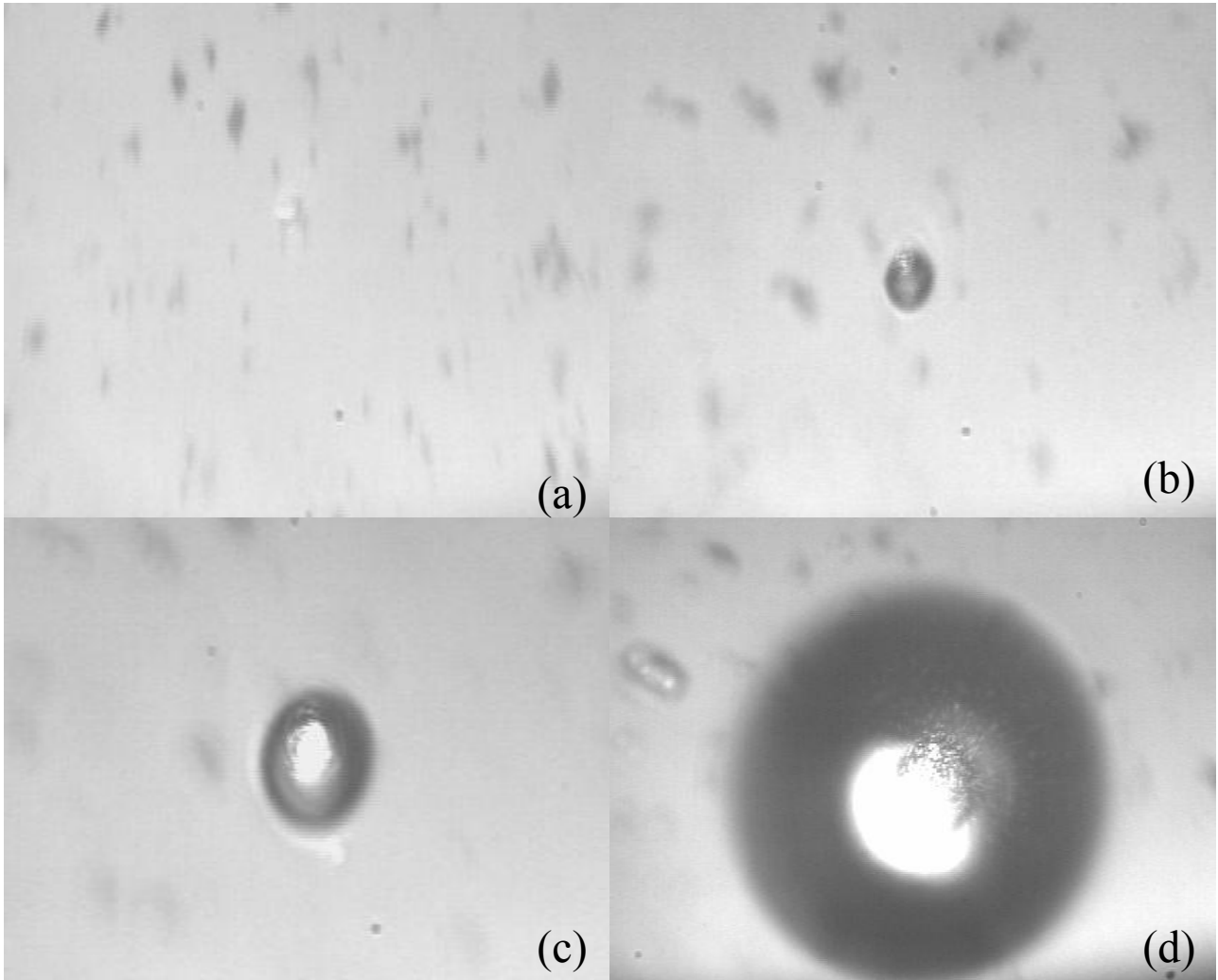


FIG 5. Microscopic images of the formation progress of light induced agglomeration by a Verdi laser at 50 mW. (a) Beginning of the trapping and agglomeration process, there are more aggregates ($1\sim 2\ \mu\text{m}$) in the center region. (b) $t=15\ \text{s}$ after the illuminations, more aggregates about $1\sim 2\ \mu\text{m}$ are attracted and deposit to the bottom of solution; (c) ($t=20\ \text{s}$) The agglomerate forms suddenly, the small aggregates in the peripheral region in (b) are sucked quickly into the center of the laser beam and left blank there. This makes the figure clean in about a radius = $50\ \mu\text{m}$ region. The forming agglomerate continues to attract aggregates from solution. (d) ($t=60\ \text{s}$) Final state of the agglomerate, almost all the small aggregates deposited on the glass slide ($1\sim 2\ \mu\text{m}$) are attracted into the donut-shaped agglomerate and the entire screen is cleaned. A convex lens was used to result a circular shaped microstructure.

Agglomeration began to take place when the laser beam was shifted a few micrometers to the peripheral region of the collected aggregates. We observed that the GNAs as far as 100 micrometers away were sucked into the agglomeration region and began to form a ring microstructure (FIG 5c). Eventually, on the time scale of 1-5 minutes, a large circular, donut-shaped microstructure with an outer diameter approximately 60 microns was formed and the hole in the center had a diameter of about $15\ \mu\text{m}$, and it became stabilized (FIG 5d). The bright spot in the center of the agglomerate was the focal spot of the laser beam. After the donut-shaped microstructure was fully grown and the laser beam was blocked, it would be stable for 10-20 minutes before it eventually broke apart or redispersed into smaller aggregates or nanoparticles again. This photo-induced agglomeration process was easily reproducible. Occasionally, the microstructure was stable for longer periods of time. If one of these stable samples was left to dry, a disk of gold nanoparticles/aggregates with a hole in the center could be clearly observed on the glass substrate under a microscope.

Meanwhile, when the power of the laser beam is increased, the size of this agglomerate structure increased accordingly as well as the speed of forming the agglomerate.

Possible manipulation of the agglomerate with a laser beam was also investigated. After the formation of the agglomerate, if the glass slide was moved laterally by 2-5 μm , the metal agglomerate initially moved together with the glass slides, then jumped rapidly to the shifted new focal point, showing that it was trapped. The agglomerate did not follow if the laser beam was moved farther away (e.g., $\sim 20 \mu\text{m}$).

D. Measurement of Electrical Conductivity of Gold Aggregates Solution

It observed that when the GNAs solution was illuminated with a laser beam at 532 nm, the electrical conductivity of the solution increased quite drastically (FIG 6). During the illumination, the temperature of the solution increased from 30 $^{\circ}\text{C}$ to 50 $^{\circ}\text{C}$ in 5 minutes while the electrical current increased from 15 μA to 22 μA , indicating an increase of the electrical conductivity of the solution.

To determine if the conductivity increase was due to heating as a result of laser illumination, a hot plate was utilized as a direct heat source. The current was found to increase from 15 μA to 18 μA when the solution temperature was changed from 30 $^{\circ}\text{C}$ to 50 $^{\circ}\text{C}$ (FIG 6).

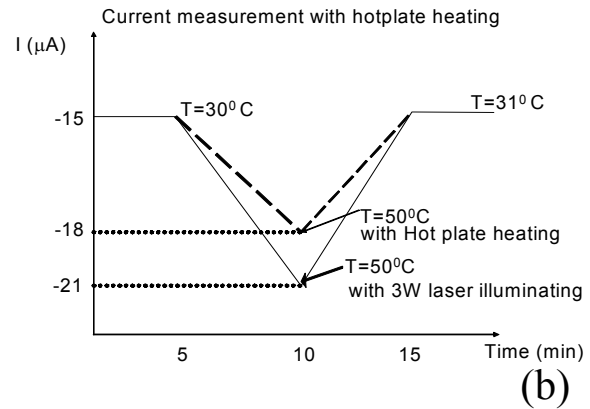


FIG 6. Comparing the current of the gold nanoparticle aggregates solution heated by the hot plate and by laser illumination. The temperature is monitored to provide the same experimental conditions for the two cases.

4. Discussion

The observed light induced further agglomeration phenomena are attributed to two processes. First, the GNAs are attracted into the central region of the laser beam. Second, stable agglomerate composed of GNAs is formed. In what follows, we first analyze the forces involved in the first process, then discuss the mechanism of forming a stable agglomerate²⁴.

A. Optical trapping force

Radiation force is usually involved in the optical trapping of particles. It will extend to a distance approximately twice the size of the beam waist. For micron-sized metal particles, ray-optics model can be used to evaluate the radiation force and multiple internal reflections do not need to be considered because of the strong absorption of the metal. For the large agglomerates we observed, the size is about 40~50 times larger than the beam waist ($w = 1 \mu\text{m}$), it will not be adequate to consider only the optical trapping force.

B. Drag force

Another force involved in the photo-induced agglomeration is the hydrodynamic drag force when the GNA solution is locally heated leading to a circulation of the fluid. In the GNAs solution, if there is a 2 μm GNA locating in the beam center, it will absorb most of the laser energy, and this amount of energy will be transferred to heat and heat the GNA to a high temperature (300~400 $^{\circ}\text{C}$)⁴¹ and this amount of energy will be finally relaxed into the water. Considering the laser power of 50 mW, if all of the energy is used to heat up the area occupied by this GNA, the hot GNA will vaporize the surrounding water. This vaporization will create a vacuum about 2 μm in diameter and the surrounding solution will flow into this area with a certain speed to fill the vacuum.

In the GNA solution, if there is a relative movement between the GNAs and the water, there will be a force exerted on the GNAs. This force will depend on the relative moving speed, shape, surface roughness of the GNAs, and the density of water

$$F_d = \frac{1}{2} C_d A \rho v^2 \quad (1)$$

where, C_d is the drag coefficient (0.47 for spherical particle), A is the cross sectional area perpendicular to the water flow, ρ is the density of the water, v is the velocity of the medium. Thus in order to calculate the drag force, one need to know the moving velocity of the surrounding water. Based on the assumption above, one can numerically calculate the fluid movement velocity in FIG 7 (a) (Fluent), and the corresponding drag force in FIG 7 (b).

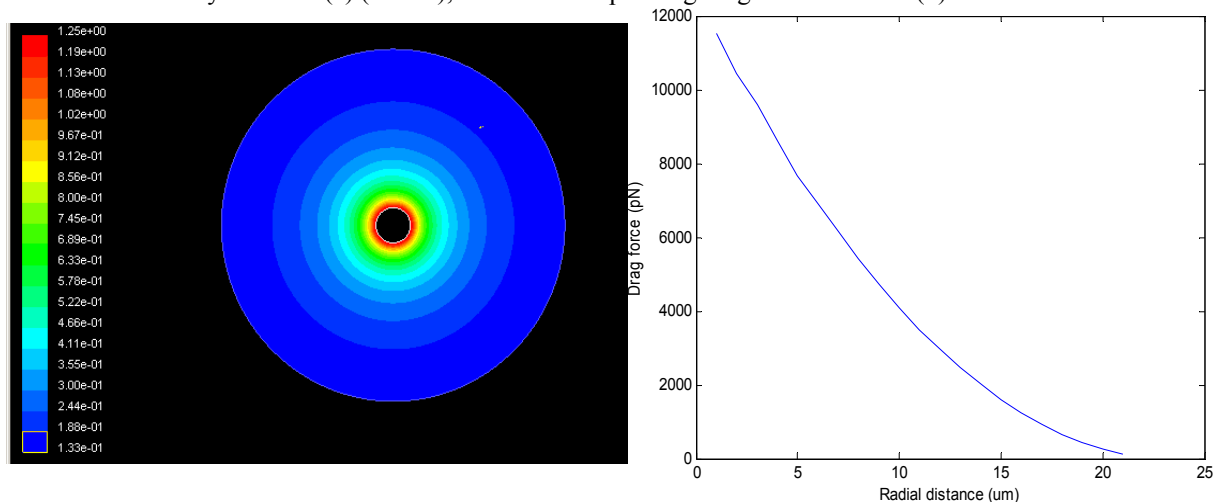


FIG 7. (a) Contour plot of the water velocity around a spherical GNA. The diameter of the GNA is 2 μm . (b) the drag force calculated according to the velocity plot in (a).

C. Radiometric Force

The light induced heating results in the radiometric force⁴⁴⁻⁴⁶ that is another important factor in the observed trapping and agglomeration. The metal nanoparticles inside the trapping beam will be heated non-uniformly due to the non-uniform intensity distribution of the Gaussian beam. The particles in the higher intensity region (near the beam center) are heated to a higher temperature, therefore they move faster, recoil back, are pushed out of the focus.⁴⁴ Previously, levitation by radiometric forces was observed with glycerol spheres that were impregnated with dye in air at low pressure.⁴⁴ For metal particles the absorption coefficient is large, especially for gold and silver at 532 nm, and radiometric force is thus expected to be strong. The radiometric force³⁷⁻³⁹ is generally repulsive. As a result, particles/aggregates will be repelled from the center of the laser focus. This explains our observation (shown in FIG 4) that a micron-sized GNA can only be trapped at the peripheral region of the laser focus spot. Also it helps to explain the hole in the donut-shaped agglomerate.

D. Mechanism of stable agglomeration

The GNAs consists of many 5-10 nm nanoparticles as the fundamental components (FIG 3). The surface chemistry of the Au particles is quite complex and not well understood. However, it has been suggested that the capping layer of the gold nanoparticles/aggregates partially consists of negatively charged ions containing sulfur and oxygen that stabilizes the nanoparticles/aggregates.⁴² Any removal of these negatively charged surface ions would destabilize the nanoparticles/aggregates and result in agglomeration due to reduced charge screening.

Due to its strong optical absorption at the laser wavelength used and the high intensity of the focused laser beam, the nanoparticles/aggregates quickly convert the light energy into thermal energy, initially resulting in a substantial increase in the local temperature of the particles. This quick and substantial increase in temperature could liberate a significant amount of capping ions from the particle surface. We suggest that when the aggregates are heated by the laser beam, the negative charged surface ions will be removed

If there are ions detached from the GNAs surface, one could expect a change in the electrical conductivity of the nanoparticle/aggregate solution upon laser illumination due to ions released from the particle surface. To test this idea, the electrical conductivity change of the metal nanoparticle/aggregate solution has been measured (FIG 6).²⁴ As expected, a noticeable increase in the conductivity (current) was measured upon light illumination of the nanoparticle/aggregate solution. The temperature of the solution was monitored at the same time and found to increase with the laser illumination. The increase in global (solution) temperature alone could increase the ion mobility and hence solution conductivity. In order to decouple the effect of global heating (averaged for the entire solution sample)

from that of local heating (nanoparticles/aggregates heated by the laser light directly before equilibrating with the entire solution), a similar experiment was performed with direct heating without light.

By heating the solution on a hot plate, we examined the effect of global heating on ion mobility in solution and possible ion liberation from the nanoparticles/aggregates, both of which can contribute towards the solution conductivity change. As shown in FIG 6, the conductivity clearly increased with heating of the solution in the same temperature range as in the laser illumination experiment (30-50 °C). However, the increase in conductivity due to thermal heating by the hot plate is noticeably less than that due to laser illumination. The difference between the two measurements is likely due to the liberation of capping ions from the particle surface by laser-induced heating, which results in a local temperature of the particles much higher than the average temperature measured for the entire solution by a thermometer.

In the case of direct thermal heating by a hot plate, ion mobility is expected to increase with the increased temperature, which results in an increase of the conductivity or current. Liberation of capping ions from the nanoparticle/aggregate surface is possible but not very significant within the temperature range under study.⁴² Therefore, the increase in ion mobility is suggested as the predominant factor in the observed increase in conductivity with heating.

In the case of laser illumination, the average solution temperature increase was the same as in the thermal heating experiment. One would expect the same conductivity increase if the effect of the laser is the same as direct thermal heating. The fact that the conductivity increase is noticeably more with laser illumination than with thermal heating suggests that additional contributions must be taken into account. One possible explanation is that, besides heat generated from the laser, direct detachment or liberation of ions is induced by photoexcitation. Another possible explanation is that the local temperature of the nanoparticles/aggregates might be much higher with the initial light absorption than the average temperature measured using a thermometer globally. A higher local temperature would also result in the release of more ions from the particle surface. The liberation from the particle surface, due to direct photoexcitation or photoinduced local heating, was consistent with the larger increase in conductivity or current in the laser illumination experiment. Very importantly, this explanation is consistent with the light-induced agglomeration observed, since ion liberation from the surface of nanoparticles/aggregates is expected to result in the formation of agglomerates.

Another possible force involved in the photo-induced agglomeration is the static electrical attractive force between oppositely charged particles. The surface chemistry of the GNAs is complicated and not well known, besides the negatively charged sodium chloride, there are also some positively charged ions on the surface of and inside the GNAs. Due to the heating effect, if the negatively charged ions are removed, the GNAs left in the beam central region may be positively charged. On the other hand, the aggregates far away are still negatively charged. According to Coulomb's law, one would expect an attractive force between the aggregates in the beam center and those far away from the beam center. In that case, the amount of the static electric force depends on the amount of negatively charged ions knocked off the GNAs surface. To verify this possibility, further study about the surface chemistry of the GNAs is necessary.

5. Conclusion

The optical trapping of micron-sized metal gold nanoparticle aggregates (GNAs) with a TEM₀₀ mode laser light at 532 nm has been demonstrated. Besides the successful optical trapping of 1-3 μm GNAs, an unusual light-induced agglomeration of GNAs has also been observed. By illuminating the nanoparticles with a 50 mW focused laser beam, a 60-100 μm donut-shaped metal microstructure was formed in a GNA solution. The size of the agglomerate microstructure is proportional to the power of the laser. This agglomeration phenomenon, along with optical trapping of the nanoparticles/aggregates, was analyzed by considering the radiation force and the radiometric force, as well as the hydrodynamic drag force caused by the laser heating. The observed conductivity changes of the nanoparticle/aggregate solution upon light illumination supports the suggestion of photothermal ion detachment. The results indicate the possibility of using light to control the surface properties of nanomaterials and thereby to design and fabricate microstructures from nanomaterials for device applications in nanotechnology.

6. Acknowledgement

This research is supported by the National Science Foundation (ECS-0401206 and CHE-0456130), and by University of California at Santa Cruz, Special Research Grants.

7. References

1. P. B. Johnson and R. W. Christy "Optical constants of Noble Metals" Phys. Rev. B. **1972**, 6, pp 4370-4379
2. M. Kerker, "The Optics of Colloidal Silver: Something Old and Something New" J. Colloid Interface Sci. **1985**, 105, pp 297-314
3. M. Quinten, "Optical constants of gold and silver clusters in the spectral range between 1.5eV and 4.5 eV" Z. Phys. **1996**, B 101, pp 211-217
4. K. L. Kelly, Eduardo, L. Zhao, G. C. Schatz "The optical Properties of Metal Nanoparticles: The Influence of Size, Shape, and Dielectric Environment" J. Phys. Chem. B. **2003**, 107, pp 668-677
5. A. M. Schwartzberg, C. D. Grant, A. Wolcott, C. Talley, T. Huser, R. Bogomolni, J. Z. Zhang, "Novel gold nanoparticle aggregates for surface-enhanced Raman scattering" J. Phys. Chem. B, **2004**, 108, pp 19191-19197
6. T. J. Norman, Jr. C. D. Grant, Donny Magana and J. Z. Zhang, J. Liu, D. Cao and F. B. Anthony Van, "Near infrared absorption of gold nanoparticle aggregates" J. Phys. Chem. B **2002** 106, pp 7005-7012
7. J. M. Gerardy and M. Ausloos "Absorption spectrums of clusters of spheres from the general solutions of Maxwell's equations II. Optical properties of aggregated metal particles" Phys. Rev. B. **1982**, 25, pp 4204-4229
8. M. P. J. van Staveren, H. B. Brom and L. J. de Jongh, "Physical properties of metal properties of metal cluster compounds II: DC- conductivity of the high nuclearity gold cluster compound" Sol. Sta. Comm. **1986**, 60, pp 319-322
9. J. J. Mock, B. D. R. Smith, D. A. Schultz and S. Scheltz, "Shape effects in plasmon resonance of individual colloidal silver nanoparticles" J. Chem. Phys. **2002**, 116, pp 6755-6759
10. M. Moskovits, "Surface-enhanced spectroscopy" Rev. Mod. Phys. **1985**, 57, pp 783-826
11. K. Kneipp, H. Kneipp, I. Itzkan, R. R. Dasari, M. S. Feld. "Surface-enhanced Raman scattering and biophysics" J. Phys.-Condes. Matter, **2002**, 14, pp R597-624
12. P. Kambhampati, C. M. Child, M. C. Foster and A. Campion, " On the chemical mechanism of surface enhanced Raman scattering: Experiment and theory" J. Chem. Phys. **1998**, 108, pp 5013-5026
13. K. Kneipp, H. Kneipp, I. Itzkan, R. R. Dasari, M. S. Feld, "Ultrasensitive chemical analysis by Raman spectroscopy" Chem. Rev. **1999**, 99, pp 2957-2976
14. A. Campion and P. Kambhampati, "Surface enhanced Raman scattering" Chem. Soc. Rev. **1998**, 27, pp 241-250
15. A. Otto, "Theory of First Layer and Single Molecule Surface Enhanced Raman Scattering (SERS)" Phys. Stat. Sol. (a) **2001**, 188, pp 1455-1470
16. B. J. Messinger, K. U. vonRaben, R. K. Chang, P. W. Barber "Local fields at the surface of noble-metal microspheres" Phys. Rev. B **1981** 24, pp 649-657
17. F. J. Garcia-Vidal and J. B. Pendry, "Collective Theory of Surface Enhanced Raman Scattering" Phys. Rev. Lett. **1996**, 77, pp 1163-1166
18. M. Quinten, "Optical Effects Associated with Aggregates of Cluster" J. Cluster Sci. **1999**, 10, pp 319-358
19. M. Quinten, "Local fields close to the surface of nanoparticles and aggregates of nanoparticles" Appl. Phys. B **2001**, 73, pp 245-255
20. A. M. Michaels, J. Jiang, L. Brus, "Ag Nanocrystal Junctions as the Site for Surface-Enhanced Raman Scattering of Single Rhodamine 6G Molecules" J. Phys. Chem. B **2000**, 104, pp 11965-11971
21. A. N. Shipway, M. Lahav, R. Gabai and I. Willner, "Investigations into the Electrostatically Induced Aggregation of Au Nanoparticles" Langmuir, **2000**, 16, pp 8789-8795
22. M. Quinten and U. Kreibig, "Absorption and elastic scattering of light by particle aggregate"s Appl. Opt. **1993**, 32, pp 6173-6182
23. S. Nahal, H. R. M. Khalesifard, J. Mostafavi-amjadl, "Photothermal-induced dichroism and micro-cluster formation in Ag⁺-doped glasses" Appl. Phys. B **2004**, 79, pp 513-518
24. Y. Zhang, C. Gu, A. Schwartzberg, S. Chen and J. Zhang "Optical Trapping and Light Induced Agglomeration of Gold Nanoparticle Aggregates" submitted to Phys. Rev. B 2005
25. A. Ashkin, "Force of single-beam gradient laser trap on a dielectric sphere in the ray optics regime" Biophys. J **1992** 61, pp 569-582
26. A. Ashkin, "History of optical trapping and manipulation of small neutral particle, atoms, and molecules" J. IEEE Sel. Top. Quant. Elect. **2000**, 6, pp 841-856

27. P. Jordan, J. Cooper, G. Mcnay, F. T. Docherty, D. Graham, W. E. Smith, G. Sinclair and M. J. Padgett. "Surface-enhanced resonance Raman scattering in optical tweezers using co-axial second harmonic generation" *Opt. Exp.* **2005**, 13, pp 4148-4153
28. H. Furukawa and I. Yamaguchi, "Optical trapping of metallic particles by a fixed Gaussian beam" *Opt. Lett.* **1998**, 23, pp 216-218
29. K. Svoboda and S.M. Block, "Optical trapping of metallic Rayleigh Particles" *Opt. Lett.* **1994**, 19, pp 930-932
30. S. Sato, Y. Harada, Y. Waseda, "Optical trapping of microscopic metal particles" *Opt. Lett.* **2004**, 19, pp 1807-1809
31. M. Gu and D. Morrish, "Three dimensional trapping of Mie metallic particles by the use of obstructed laser beam" *J. App. Phys.* **2002**, 91, pp 1606-1612
32. H. Rubinsztein-Dunlop, T. A. Nieminen, M. E. J. Friese and N. R. Heckenberg, "Optical trapping of absorbing particles" *Adv. Quan. Chem.* **1998**, 30, pp 469-492
33. G. Roosen and C. Imbert, "The TEM_{01} Mode laser beam- A powerful tool for optical levitation of various types of spheres" *Opt. Comm.* **1978**, 26, pp 432-436
34. P. C. Ke and M. Gu "Characterization of trapping force on metallic Mie particles" *App. Opt.* **1999**, 38, pp 160-167
35. J. P. Barton, D. R. Alexander, and S. A. Schaub, "Theoretical determination of net radiation force and torque for a spherical particle illuminated by a focused laser beam" *J. App. Phys.* **1989**, 66, pp 4594-4602
36. J. P. Barton and D. R. Alexander, "Fifth-order corrected electromagnetic field compinents for a fundamental Gaussian Beam" *J. Appl. Phys.* **1989**, 66, pp 2800-2802
37. Y. Zhang, C. Gu, A. Schwartzberg, S. Chen and J. Zhang "Optical Trapping and Light Induced Agglomeration of Gold Nanoparticle Aggregates" submitted to *Phys. Rev. B* 2005
38. J. Turkevich, P. L. Stevenson, J. Hillier, *Faraday Soc* 1951, 55 pp 234
39. P. C. Lee, D. Meisel, "Adsorption and surface-enhanced Raman of dyes on silver and gold sols" *J. Phys. Chem.* **1982**, 86, pp 3391-3395
40. T. Norman, Jr., C. Grant, D. Magana, R. Anderson, J. Z. Zhang, D. Cao, F. Bridges, J. Liu, and T. van Buuren, "Longitudinal plasma resonance shifts in gold nanoparticles aggregates" *SPIE Proc.* **2002**, 4807, pp 51-58
41. C. D. Grant, A. Schwartzberg, T. Norman, Jr., J. Z. Zhang, "Ultrafast electronic relaxation and coherent vibrational oscillations of strongly coupled gold nanoparticle aggregates" *J. Am. Chem. Soc.*, **2003** 125, pp 549-553
42. M. Hu, G. V. Hartland, "Heat Dissipation for Au Particles in Aqueous Solution: Relaxation Time versus Size" *J. Phys. Chem. B* 2002, 106, pp 7029-7033
43. Yi Zhang, Adam M. Schwartzberg, Kevin Xu, Claire Gu, Jin Z. Zhang "Electrical and thermal conductivities of gold and silver nanoparticles in solutions and films and electrical field enhanced Surface-Enhanced Raman Scattering (SERS)" *Proc. SPIE* **2005**, Vol. 5929, pp. 193-201
44. M. Lewittes, S. Arnold and G. Oster, "Radiometric levitation of micro sized spheres" *Appl. Phys. Lett.* **1982** 40, pp.455
45. S. Arnold, A. B. Pluchino, K. M. Leung, "Influence of surface-mode-enhanced local fields on photophoresis" *Phy. Rev. A.* **1984** 29, pp. 654
46. S. Arnold and M. Lewittes, *J. Appl. Phys.* "Size dependence of the photophoretic force" **1982**, 53, pp 5314